01.1;01.4;06.1;13.1

Wave Functions and Energy Levels Taking into Account the Surface Potential in a Helicoidally Twisted Nanoribbon for Schrödinger Particles

© S.N. Skryabin, Y.A. Petrova, N.R. Sadykov

Snezhinsk Physics and Technology Institute, National Research Nuclear University, „MEPhI“, Snezhinsk, Russia
E-mail: stepan.skryabin.04@mail.ru

Received March 6, 2023
Revised March 18, 2024
Accepted April 22, 2024

For the narrow staggered armchair-edge graphene nanoribbons investigated the influence of the surface potential on the parameters of the stationary states of the charge carriers in vicinity of the Dirac point. For this, algorithms for searching for energy eigenvalues and eigenfunctions of stationary states in the transverse and longitudinal directions are implemented. It follows from the calculations results that, depending on the parameters of the nanoribbon, a situation is possible when its elastic properties disappear.

Keywords: four-point unit cell, surface potential, nanoribbons of the armchair type, surface energy, the inverse iteration method, energy levels of stationary states.

DOI: 10.61011/TPL.2024.08.58914.19547

Graphene is a material for unique nanostructures that are regarded, by analogy with solids, as continuous media. The parameters of such media are characterized within the theory of elasticity: Young's modulus, Poisson's ratio, torsional angle, strain tensor, stress tensor, etc. These mechanical characteristics of graphene may be used in the design of various sensors. For example, its weak resistance to bending may help construct highly sensitive pressure sensors.

Surface potential is one of the effects manifested in nanoparticles. The possibility of application of the surface potential, which allows one to study the influence of curvature in the context of low-dimensional systems, in quantum mechanics has garnered recent interest. Physical effects induced by surface curvature in the presence of an external magnetic field were investigated in [1–3] based on the Schrödinger equation for a spinless electron gas. In [1,2], a spinless electron gas was confined by a two-dimensional localized cone surface; in [3], position-dependent mass effects were examined in the case of electronic transport in curved two-dimensional quantum systems (the formalism was applied to deformed nanotubes).

In the present study, the free energy of a twisted nanoribbon due to elastic deformations is determined. The two-dimensional Schrödinger equation is used to analyze the influence of the surface potential on the free energy of a twisted nanoribbon, which in turn suppresses torsional oscillations of the nanoribbon. The results of mathematical modeling and numerical calculations based on theoretical data are presented.

According to [4], the expression for surface potential energy in a three-dimensional curvilinear coordinate system

$$\mathbf{R}(q^1, q^2q^3) = \mathbf{r}(q^1, q^2) + q^3\hat{\mathbf{N}}(q^1, q^2) \qquad (1)$$

takes the form

$$V_S = -\frac{\hbar^2}{8m_e}\left[\frac{1}{f^2}\left(\frac{\partial f}{\partial q^3}\right)^2 - \frac{2}{f}\frac{\partial^2 f}{\partial (q^3)^2}\right]\Bigg|_{q^3=0}$$
$$= -\frac{\hbar^2}{2m_e}(M^2 - K) = -\frac{\hbar^2}{8m_e}(\lambda_1 - \lambda_2)^2, \qquad (2)$$

where m_e is the electron mass; V_S depends on purely geometric parameters of two-dimensional surface $\mathbf{r}(q^1, q^2)$; $\hat{\mathbf{N}}(q^1, q^2)$ is a unit normal to the surface at the point in question; and $\mathbf{R}(q^1, q^2q^3)$ is the radius vector of points in a small neighborhood of the examined surface. In (2), $f = \sqrt{G/g}$; G and g are the determinants of metric tensors $G_{ij} = (\partial\mathbf{R}/\partial q^i)(\partial\mathbf{R}/\partial q^j)$ and $g_{\alpha\beta} = (\partial\mathbf{r}/\partial q^\alpha)(\partial\mathbf{r}/\partial q^\beta)$, respectively; $dS = \sqrt{g}dq^1dq^2$ is the elementary area of a two-dimensional surface; $dV = \sqrt{G}dq^1dq^2dq^3$ is the elementary volume; and λ_1 and λ_2 are the principal curvatures specifying mean curvature M and Gaussian curvature K [5] of the surface and are the solutions of equation [5,6]

$$\begin{vmatrix} b_{11} - \lambda g_{11} & b_{12} - \lambda g_{12} \\ b_{21} - \lambda g_{21} & b_{22} - \lambda g_{22} \end{vmatrix} = 0. \qquad (3)$$

In (3), metric tensor $g_{\alpha\beta}$ of a two-dimensional surface and second-rank tensor of dimension two $b_{\alpha\beta}$ are the first and second quadratic forms [5], respectively. According to [4], surface potential V_S in (2) emerges as a result of decomposition of term $[-\hbar^2/(2m_e)]\Delta$ in the three-dimensional Schrödinger equation into a surface part for q^1, q^2 and a normal part for q^3 (Δ is the three-dimensional Laplace operator). In passing to the two-dimensional Schrödinger equation (two-dimensional surface), surface potential V_S arises out of the fact that the two-dimensional Laplace operator gets corrected by $\delta\Delta_\perp = -(\lambda_1 - \lambda_2)^2/4$. It follows from (2) that the surface potential at any point

on a surface is always either negative or equal to zero. This implies that the introduction of this term into the two-dimensional Schrödinger equation results in lowering of the energy level of stationary states. Since the deformation of a surface by elastic forces (by analogy with elastic forces in deformation of metal plates) raises the potential energy of plates, surface potential V_S from (2) competes with transverse elastic deformations. This effect is especially strong when principal curvatures λ_1 and λ_2 of a surface differ significantly (e.g., when $\lambda_2 = 0$ (cylinder) or $\lambda_1 = -\lambda_2$ (helicoid)).

Using the first $g_{\alpha\beta}$ and second $b_{\alpha\beta}$ quadratic forms in the helicoidal coordinate system given in [7] and taking into account the surface potential for particles characterized by the Schrödinger equation [4,8,9], we obtain an equation for the wave function of a particle in a longitudinal electric field W:

$$-\frac{\hbar^2}{2m_e}\left[\frac{\partial^2}{\partial(q^1)^2}+\frac{\kappa^2 q^1}{1+(\kappa q^1)^2}\frac{\partial}{\partial q^1}+\frac{\kappa^2}{[1+(\kappa q^1)^2]^2}\right]\Psi$$

$$-\frac{\hbar^2}{2m_e[1+(\kappa q^1)^2]}\frac{\partial^2}{\partial(q^2)^2}\Psi=(E-E_{\mathrm{F}}+|e|Wq^2)\Psi. \quad (4)$$

In the present study, we examine narrow long armchair-edge graphene nanoribbons (N-AGNR) with a staggered configuration (Fig. 1), where $N = 11$ [10,11]. At $\kappa q^1_{\max} \ll 1$, nanoriboon width $H = m\sqrt{3}b \approx 1.23\,\mathrm{nm}$ for $m = (N-1)/2 = 5$ ($b = 0.142\,\mathrm{nm}$ is the distance between carbon atoms in graphene), and helicoidal nanoribbon period $L = 10H$, we obtain $[1+(\kappa q^1_{\max})^2] \approx 1.05$, where $q^1_{\max} = H/2$, $\kappa L = 2\pi$. Therefore, Eq. (4) may be approximately solved numerically by the method of separation of variables $\Psi = \Phi_1(q^1)\Phi_2(q^2)$ with boundary conditions $\Phi_2(q^2 = \pm 5L) = 0$, $\Phi_1(q^1 = \pm 5H) = 0$:

$$\frac{\partial^2}{\partial(q^2)^2}\Phi_2 = -\frac{2m_e}{\hbar^2}(E-E_1+|e|Wq^2)\Phi_2,$$

$$\left[\frac{\partial^2}{\partial(q^1)^2}+\frac{\kappa^2 q^1}{1+(\kappa q^1)^2}\frac{\partial}{\partial q^1}+\frac{\kappa^2}{[1+(\kappa q^1)^2]^2}\right]\Phi_1$$

$$= -\frac{2m_e}{\hbar^2}(E_1-E_{\mathrm{F}})\Phi_1, \quad (5)$$

where L and H are the length and width of a nanoribbon and E are the energy levels of stationary states, which include the energy levels in longitudinal $(E-E_1)$ and transverse (E_1-E_{F}) directions. The solution for function Φ_2 from the first equation in (5) may also be expressed in terms of Airy functions $\mathrm{Ai}(\xi)$ and $\mathrm{Bi}(\xi)$ [12,13].

Let us now determine the influence of the surface potential on free energy $\widetilde{\mathscr{F}}$ of a twisted nanoribbon. The value of $\widetilde{\mathscr{F}}$ is the difference between the energy levels of stationary states of twisted $E_n(\kappa)$ and flat $E_n(\kappa = 0)$ nanoribbons:

$$\widetilde{\mathscr{F}} \sim \Delta E = [E_n(\kappa)-E_{\mathrm{F}}]-[E_n(\kappa=0)-E_{\mathrm{F}}]$$

$$= E_n(\kappa)-E_n(\kappa=0).$$

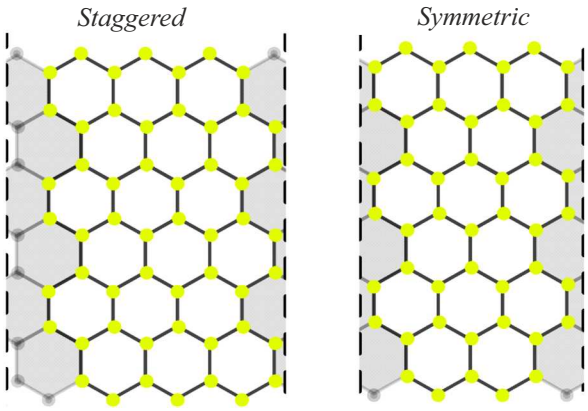

Figure 1. Images of armchair-edge nanoribbons with staggered and symmetric configurations.

Since the first equation for function Φ_2 from system (5) does not depend on torsional parameter κ, energy level difference ΔE is governed by the magnitude of energy level difference in the transverse direction $\Delta E_1 = E_{1,n}(\kappa) - E_{1,n}(\kappa = 0)$ for function Φ_1 from (5):

$$\widetilde{\mathscr{F}} = \widetilde{F}L = [4HL/(3\sqrt{3}b^2)]\Delta E \approx [4HL/(3\sqrt{3}b^2)]\Delta E_1, \quad (6)$$

where $\Delta E \approx \Delta E_1 < 0$ and the expression in square brackets defines the number of carbon atoms in a nanoribbon. Since the second and third terms in square brackets in (5), which act as a perturbation operator, are proportional to κ^2, energy correction ΔE_1 is also proportional to κ^2.

Let us now determine the free energy of a twisted nanoribbon due to elastic deformations in the case when this nanoribbon is approximated by a long narrow thin elastic plate with its elastic parameters being well known [14–16]. To do this, we apply the theory of deformation of thin rods with a rectangular cross section to nanoribbons [17]. In the case of torsional deformation, a rod remains straight, but each cross-section is rotated relative to the underlying ones by angle $d\varphi = \tau\, dz$, where τ is the torsional angle. The torsional deformation itself (i.e., relative displacements of adjacent sections of the rod) is assumed to be small. This is achieved if the relative rotation of cross sections separated longitudinally by distances on the order of transverse dimensions R of the rod is small; i.e., $\tau R \ll 1$. Let us introduce components u_x, u_y of the displacement vector and strain u_{ik} and stress σ_{ij} tensors:

$$u_x = -\tau zy, \quad u_y = \tau zx, \quad u_z = \tau\psi(x,y),$$

$$u_{ik} = \frac{1}{2}(\partial u_i/\partial x_k + \partial u_k/\partial x_i), \quad (7)$$

$$\sigma_{ij} = \frac{E}{1+\sigma}\left(u_{ij}-\frac{1}{3}u_{ll}\delta_{ik}\right)+u_{ll}\delta_{ik}K$$

$$= \frac{E}{1+\sigma}\left(u_{ij}+\frac{\sigma}{1-2\sigma}u_{ll}\delta_{ik}\right), \quad (8)$$

where $\psi(x, y)$ is the torsional function and $u_{ll} = 0$ is pure shear deformation. In the case of a thin plate, the non-zero components are σ_{xz}, σ_{yz} [17], which may be expressed through auxiliary function $\chi(x, y)$:

$$\sigma_{xz} = 2\mu\tau\,\frac{\partial\chi}{\partial y}, \qquad \sigma_{yz} = -2\mu\tau\,\frac{\partial\chi}{\partial x}, \tag{9}$$

where $\mu = E/[2(1+\sigma)]$ is the shear modulus. With (9) taken into account, we find the equation for function χ

$$\Delta\chi = \partial^2/\partial x^2 + \partial^2/\partial y^2 = -1. \tag{10}$$

The free energy of mechanical deformations (F) per unit volume of a twisted rod is

$$F = \frac{\sigma_{ij}u_{ik}}{2} = \frac{1}{2\mu}\left[(\sigma_{xz})^2 + (\sigma_{yz})^2\right] = 2\mu\tau^2(\mathrm{grad}\,\chi)^2. \tag{11}$$

Torsional rigidity C of the rod provides an opportunity to define torsional energy (free energy) $\mathscr{F}$ without including the surface potential

$$\mathscr{F} = L\int F df = LC\tau^2/2,$$

$$C = 4\mu\int(\mathrm{grad}\,\chi)^2 df = \frac{\mu H a^3}{3}, \tag{12}$$

where integration is performed over the cross-sectional area of the rod.

With the surface potential taken into account, the equation for torsional vibrations of a nanoribbon is written as

$$\frac{\partial^2\varphi}{\partial t^2} = \frac{C + C_{sp}}{\rho I}\,\frac{\partial^2\varphi}{\partial z^2}, \qquad C_{sp} = -\left[\frac{8H}{3\sqrt{3}b^2\kappa^2}\right]\Delta E,$$

$$v_{sp} = \sqrt{\frac{C + C_{sp}}{\rho I}}, \qquad \omega_{sp} = \frac{\pi v_{sp}}{L}, \tag{13}$$

$$C = \frac{2\mathscr{F}}{L\tau^2} \approx 6.84\cdot 10^{-28}\,\mathrm{J\cdot m}, \qquad (C + C_{sp})/C = 0.7, \tag{14}$$

where torsional rigidity C is calculated for nanoribbon thickness $a = 0.154$ nm; C_{sp} — parameter that characterizes the effect of the surface potential on the rod oscillation frequency.

The data on evolution of the total energy of systems examined in [18] reveal complete structural and energetic stability and confirm that these systems are highly flexible and may remain intact at relatively high temperatures, demonstrating their remarkable thermal stability. The analysis of electronic properties of nitrogen-containing carbon nanoribbons composed of 4−5−6−8-membered rings revealed that the studied systems are direct-band-gap semiconductors in nature. The estimated band gap was 1.12 eV, which is lower than the value of 1.4 eV measured experimentally in [19] for the C_{52} system. Fixed thickness and width values of these nanoribbons were adopted in the study (3.35 and 11.75 Å respectively). The predicted elastic moduli of systems C_{52}, $C_{48}N_4$-1, $C_{48}N_4$-2, $C_{44}N_8$, and $C_{40}N_{12}$ were 534, 500, 510, 473, and 493 GPa, respectively. The used approximation of a carbon nanoribbon by rods with a rectangular cross-section (directional chemical bonds are disregarded) is simplified compared to [18]. However, since the geometric dimensions of nanoribbons and the predicted elastic moduli of systems in [18] correspond to the values used here, a qualitative agreement between the theoretical results obtained and the actual parameters of nanoribbons is perfectly possible. The slight difference between the elastic modulus used in the present study and the data from [18] may be attributed to the fact that a carbon nanoribbon is more homogeneous than the nanoribbons examined in [18] (a more accurate approximation of nanoribbons by rods with a rectangular cross-section).

A series of numerical calculations were carried out to determine the energy level of stationary states and wave functions in the transverse $\Phi_1(q^1)$ and longitudinal $\Phi_2(q^2)$ directions of a nanoribbon from Eqs. (5). The profile of a shallow potential well in the transverse U_{tr} and longitudinal U_{lon} directions was considered in these calculations:

$$U_{tr} = \begin{cases} E_{\mathrm{F}}, & |q^1| \leqslant H/2, \\ 0, & H/2 < |q^1| \leqslant 5H, \end{cases} \tag{15}$$

$$U_{lon} = \begin{cases} E_1 - |e|Wq^2, & |q^2| \leqslant L/2, \\ -|e|Wq^2, & L/2 < |q^2| \leqslant 5L, \end{cases} \tag{16}$$

where $E_{\mathrm{F}} = -6.4$ eV and quantity E_1 was defined in (5). Calculations were performed on the basis of an algorithm for determining the eigenvalues and eigenfunctions of stationary states, which implements the method of inverse iterations [20] (or the modified Wielandt method [21]). Similar numerical algorithms were implemented in [22–24].

Table 1 presents calculated energy levels of stationary states $E_1 = E_{1,n}(\kappa)$ in the transverse direction for a potential well with profile (15) and energy levels of stationary states $E = E_n(\kappa)$ in the longitudinal direction for a potential well with profile (16). Figure 2 shows the dependence of the normalized functions of states in an armchair-edge nanoribbon. The data in Fig. 2, *a* correspond to the dependence of wave functions in the transverse direction on q^1 when the first boundary condition is satisfied at $q^1 = \pm 5H$ and the potential well profile is given by (15). It can be seen from Fig. 2, *a* that the probability density outside a nanoribbon at $|q^1| > H/2$ is greater than zero. The data in Fig. 2, *b* correspond to the dependence of wave functions in the longitudinal direction on q^2 when the first boundary condition is satisfied at $q^2 = \pm 5L$ and the potential well profile is given by (16). It can be seen from Fig. 2, *b* that the probability density outside a nanoribbon at $q^2 > L/2$ is virtually equal to zero.

The variation of the total free energy with nanoribbon thickness is detailed in the first row of Table 2. The second and third rows present the variations of velocity and frequency of torsional oscillations of the fundamental

Table 1. Energy levels of stationary states $E_1 = E_{1,n}(\kappa)$ in the transverse direction and $E = E_n(\kappa)$ in the longitudinal direction for potential wells with profiles (15) and (16)

State number n	Energy levels in the longitudinal direction (Fig. 2, b)		Energy levels in the transverse direction (Fig. 2, a)	
	Flat AGNR, $E_n(\kappa = 0)$, eV	Helicoidal AGNR, $E_n(\kappa)$, eV	Flat AGNR, $E_{1,n}(\kappa = 0)$, eV	Helicoidal AGNR, $E_{1,n}(\kappa)$, eV
1	−6.2297	−6.2440	−6.2039	−6.2182
2	−6.2024	−6.2166	−5.6186	−5.6418
3	−6.1800	−6.1942	−4.6538	−4.6671
4	−6.1597	−6.1740	−3.3317	−3.3545
5	−6.1386	−6.1528	−1.7062	−1.7183
6	−6.1132	−6.1275	−0.0479	−0.0645

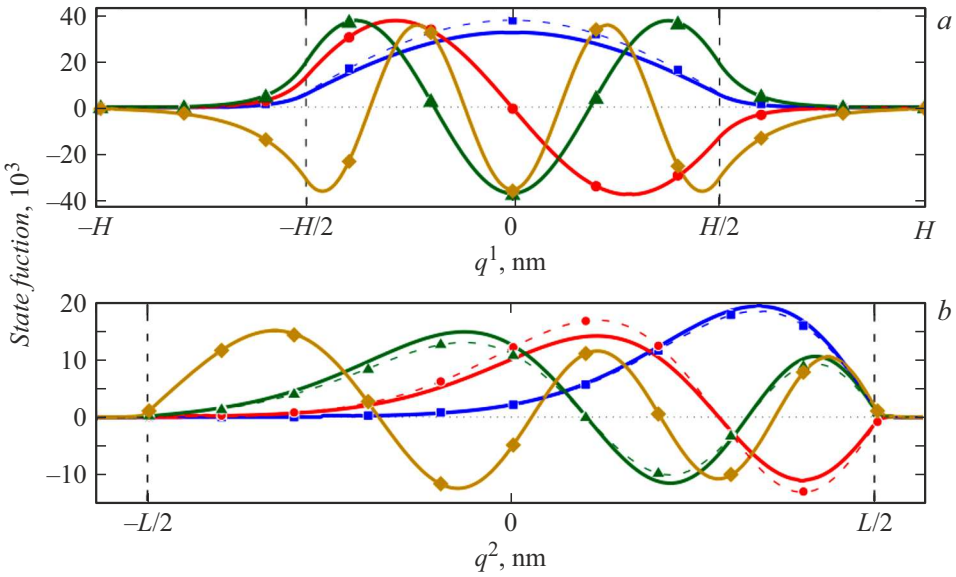

Figure 2. Dependences of normalized state functions in a nanoribbon. a — dependence of wave functions in the transverse direction on q^1 ($H = 1.23$ nm), where $|q^1| \leqslant 5H$. b — dependence of wave functions in the longitudinal direction on q^2 ($L = 12.3$ nm), where $|q^2| \leqslant 5L$. Dashed vertical lines correspond to nanoribbon edges and ends $q^1 = \pm H/2$ and $q^2 = \pm L/2$, respectively. Solid curves and dashed curves with different symbols correspond to twisted and flat ($\kappa = 0$) nanoribbons, respectively.

Table 2. Calculation of total free energy $\mathscr{F} + \mathscr{F}_{sp}$ and propagation velocity v_{sp} and cyclic frequency ω_{sp} of torsional oscillations of the fundamental mode of a helicoidal wave as functions of nanoribbon thickness a

Parameter	a/b					
	1.153	1.155	1.16	1.2	1.5	2
$\mathscr{F}+\mathscr{F}_{sp}$, eV	~ 0	0.04	0.15	1.06	10	35.1
v_{sp}, m/s	4.4	195.9	361.5	947.7	2909.1	5450.3
ω_{sp}, 10^{11} s^{-1}	0.011	0.5	0.92	2.42	7.43	13.92

mode of a helicoidal wave (determined with account for the surface potential) with nanoribbon thickness.

Figure 3 shows the dependences of the propagation velocity and the cyclic frequency of torsional oscillations of the fundamental wave mode on the value of a/b. Curves *1* in Fig. 3 correspond to the case when only the energy of elastic deformations is taken into account. Curves *2* were plotted with the energy of both elastic deformations and surface potential taken into account.

Thus, it follows from the obtained results that quantity $C + C_{sp}$ may assume a zero value. Velocity v_{sp} and frequency ω_{sp} are also zero in this case. This implies that an elastic thin narrow nanoribbon is transformed, in terms of its elastic properties, into a strip of fabric (i.e., the elastic properties of the nanoribbon vanish completely). Condition $C + C_{sp} = 0$ is fulfilled at $a/b \approx 1.1513$, where the frequency of torsional vibrations corresponds to microwave radiation with wavelength $\lambda = 1.67$ m. The oscillation frequency may be reduced by increasing the width and length of a nanoribbon, but the influence of the surface potential on the examined effect is then suppressed. It

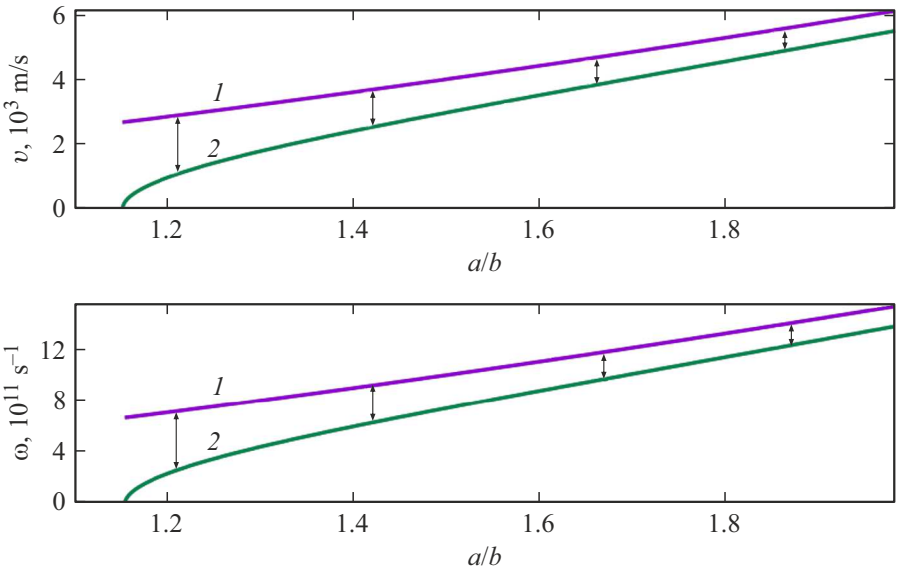

Figure 3. Dependences of the propagation velocity (upper panel) and the cyclic frequency (lower panel) of torsional oscillations of the fundamental wave mode on the value of a/b. Since velocity v is proportional to frequency ω, the functional dependences of these quantities agree qualitatively.

should be stressed that torsional rigidity C was calculated in the present study for nanoribbon thickness $a = 0.154$ nm ($a/b = 1.085$) corresponding to the data for graphene nanoribbons, while the nanoribbon thickness in [18] was $a = 0.335$ nm (i.e., $a/b = 2.36$). At $a/b = 2.36$, torsional oscillation frequency ω_{sp} approaches a stationary value; i.e., a nanoribbon does not collapse. But even though a nanoribbon does not collapse, the torsional rigidity decreases. The latter factor may prove to be significant in experimental research into the effects associated with the Young's modulus value in nanostructures.

It follows from the obtained results that the geometric potential may influence the nature of motion of charge carriers in elongated nanoparticles (nanotubes, nanoribbons). This issue is relevant to chiral spintronics [25–29]. The influence of the geometric potential will manifest itself in non-axisymmetric motion of particles in nanotubes, which translates into the influence of the geometric potential on the spin-orbit interaction magnitude [23]. In turn, the spin-orbit interaction lifts spin degeneracy in nanotubes (Rashba effect). The shift of energy levels in twisted nanoribbons should affect the transmission coefficient.

Funding

The authors would like to thank the National Research Nuclear University „MEPhI" for support provided under the Competitiveness Enhancement Program „Project 5-100" (contract No. 02.a03.21.0005.27.08.2013).

Conflict of interest

The authors declare that they have no conflict of interest.

References

[1] L.F.C. Pereira, F.M. Andrade, C. Filgueiras, E.O. Silva, Physica E, **132**, 114760 (2021). DOI: 10.1016/j.physe.2021.114760.
[2] L.F.C. Pereira, F.M. Andrade, C. Filgueiras, E.O. Silva, Annal. der Phys., **531**, 1900254 (2019). DOI: 10.1002/andp.201900254
[3] F. Serafim, F.A.N. Santos, J.R.F. Lima, C. Filgueiras, F. Moraes, Physica E, **108**, 139 (2019). DOI: 10.1016/j.physe.2018.12.022
[4] R.C.T. da Costa, Phys. Rev. A, **23**, 1982 (1981). DOI: 10.1103/PhysRevA.23.1982
[5] B.A. Dubrovin, S.I. Novikov, A.T. Fomenko, *Sovremennaya geometriya. Metody i prilozheniya*, 2nd ed. (Nauka, M., 1986) (in Russian).
[6] M. Spivak, *A comprehensive introduction to differential geometry* (Boston, 1999).
[7] N.R. Sadykov, Yu.A. Petrova, I.A. Pilipenko, R.S. Khrabrov, S.N. Skryabin, Russ. J. Phys. Chem., **97**, 367 (2023). DOI: 10.1134/S003602442302022X.
[8] R. Dandoloff, T.T. Truong, Phys. Lett. A, **325**, 233 (2004). DOI: 10.1016/j.physleta.2004.03.050
[9] V. Atanasov, R. Dandoloff, A. Saxena, Phys. Rev. B, **79**, 033404 (2009). DOI: 10.1103/PhysRevB.79.033404
[10] A. Onipko, L. Malysheva, Phys. Status Solidi B, **255**, 1700248 (2017). DOI: 10.1002/pssb.201700248
[11] R.W. Boyd, *Nonlinear optics* (Academic Press, San Diego, 2003).
[12] N.R. Sadykov, R.S. Khrabrov, I.A. Pilipenko, Eur. Phys. J. D, **77**, 9 (2023). DOI: 10.1140/epjd/s10053-022-00582-5
[13] N.R. Sadykov, R.S. Khrabrov, I.A. Pilipenko, Pis'ma Zh. Tekh. Fiz., **48** (16), 34 (2022) (in Russian). DOI: 10.21883/PJTF.2022.16.53205.19216 [N.R. Sadykov, R.S. Khrabrov, I.A. Pilipenko, Tech. Phys. Lett., **48** (8), 69 (2022). DOI: 10.21883/TPL.2022.08.55067.19216].

[14] A.V. Orlov, I.A. Ovid'ko, Rev. Adv. Mater. Sci., **40**, 249 (2015). https://www.ipme.ru/e-journals/RAMS/no_34015/05_34015_orlov.html
[15] C. Lee, J.W. Kysar, X. Wei, J. Hone, Science, **321**, 385 (2008). DOI: 10.1126/science.1157996
[16] S.K. Krishnan, E. Singh, P. Singh, M. Meyyappan, H.S. Nalwa, RSC Adv., **9**, 8778 (2019). DOI: 10.1039/c8ra09577a
[17] L.D. Landau, E.M. Lifshitz, *Teoreticheskaya fizika. Teoriya uprugosti*, 4th ed. (Nauka, M., 1987) (in Russian).
[18] B. Mortazavi, J. Compos. Sci., **7**, 269 (2023). DOI: 10.3390/jcs7070269
[19] F. Kang, L. Sun, W. Gao, Q. Sun, W. Xu, ACS Nano, **17**, 8717 (2023). DOI: 10.1021/acsnano.3c01915
[20] B.N. Parlett, *The symmetric eigenvalue problem* (Prentice-Hall, Inc., Englewood Cliffs, N.J., 1980).
[21] H. Wielandt, Math. Z., **50**, 93 (1944). DOI: 10.1007/BF01312438
[22] A.N. Afanas'ev, L.A. Myalitsin, N.R. Sadykov, M.O. Sadykova, Russ. Phys. J., **48**, 10 (2005). DOI: 10.1007/s11182-005-0078-1.
[23] L.I. Ardasheva, N.D. Kundikova, M.O. Sadykova, N.R. Sadykov, V.E. Chernyakov, Opt. Spectrosc., **95**, 645 (2003). DOI: 10.1134/1.1621451.
[24] L.I. Ardasheva, N.R. Sadykov, V.E. Chernyakov, Sov. J. Quantum Electron., **22**, 840 (1992). DOI: 10.1070/QE1992v022n09ABEH003610.
[25] S.H. Yang, Appl. Phys. Lett., **116**, 120502 (2020). DOI: 10.1063/1.5144921
[26] S.H. Yang, R. Naaman, Y. Paltiel, S.S.P. Parkin, Nat. Rev. Phys., **3**, 328 (2021). DOI: 10.1038/s42254-021-00302-9
[27] K. Michaeli, N. Kantor-Uriel, R. Naaman, D.H. Waldeck, Chem. Soc. Rev., **45**, 6478 (2016). DOI: 10.1039/C6CS00369A
[28] R. Naaman, D.H. Waldeck, Annu. Rev. Phys. Chem., **66**, 263 (2015). DOI: 10.1146/annurev-physchem-040214-121554
[29] P.N. D'yachkov, E.P. D'yachkov, Appl. Phys. Lett., **120**, 173101 (2022). DOI: 10.1063/5.008690

Translated by D.Safin